Molecular Vision 2021; 27:1-16 <http://www.molvis.org/molvis/v27/1>
Received 9 September 2020 | Accepted 4 January 2021 | Published 6 January 2021

Spectrum of germline mutations in RB1 in Chinese patients with retinoblastoma: Application of targeted next-generation sequencing

Yihua Zou, Jiakai Li, Peiyan Hua, Tingyi Liang, Xunda Ji, Peiquan Zhao

Department of Ophthalmology, Xinhua Hospital, Affiliated to Shanghai Jiao Tong University School of Medicine, Shanghai, China.

Purpose: Retinoblastoma (RB) is a pediatric ocular malignancy due to biallelic inactivation of the *RB1* gene. Genetic testing is critically important for treatment decisions for this disease. Targeted next-generation sequencing (NGS) has been demonstrated to be an effective strategy for discovering all types of mutations in the *RB1* gene. The aim of this study is the application of targeted NGS in a cohort of Chinese patients with retinoblastoma to identify germline mutations in the *RB1* gene.

Methods: Blood samples were collected from 149 unrelated probands with retinoblastoma (62 bilaterally and 87 unilaterally) and their parent(s). Genomic DNA was analyzed with custom panel-based targeted NGS, and the panel was designed to include exons 1–27 of the *RB1* gene with flanking intronic sequences. Single nucleotide variations (SNVs) and small insertions/deletions (InDels) identified were confirmed with Sanger sequencing. If the Sanger sequencing of a low-frequency variant (LFV) detected with targeted NGS was negative, PCR-based deep NGS was conducted for added confirmation. Copy number variations (CNVs) detected with targeted NGS were confirmed with multiplex ligation-dependent probe amplification (MLPA).

Results: Overall, 74 germline mutations were detected in 48.3% of the probands (72/149, 56 bilateral and 16 unilateral cases). The total detection rate in the bilateral cases was 90.3% (56/62). These mutations included 64 SNVs and InDels (25 nonsense, 20 splicing, ten frameshift, eight missense, and one synonymous variants) and ten CNVs. All CNVs were confirmed with MLPA. Twenty-four (32.4%, 24/74) variants detected were novel, including nine splicing, six frameshift, five missense, and four nonsense variants. Eight LFVs (10.8%, 8/74) were found with targeted NGS; six of which were identified with Sanger sequencing, and two were identified with PCR-based deep NGS (13.16% and 3.000% mutant rates, respectively).

Conclusions: This study expanded the spectrum of germline mutations in *RB1* using targeted NGS technology, which is a cost-saving and efficient method for genetic sequencing of retinoblastoma and may improve the molecular diagnosis of retinoblastoma.

Retinoblastoma (RB; OMIM 180200) is the most common primary ocular malignancy in childhood, originating from progenitor cells of retinal photoreceptors [1]. The incidence of retinoblastoma is constant at one case per 15,000–20,000 live births worldwide, corresponding to about 9,000 new cases every year [1,2]. The majority of retinoblastomas is initiated by biallelic inactivation of the retinoblastoma susceptibility gene, *RB1* (Gene ID:5925; OMIM 614041; NM_000321) [3,4]. The *RB1* gene is a prototypic tumor suppressor gene, and its production is a protein (pRB, NP_000312.2) with 928 residues [5,6]. The structure of pRB is divided into three domains composed of an N-terminus, an R motif and A/B "pocket," and a C-terminus [7]. The mutations in the *RB1* gene that inactivate the pRB can make the cell cycle progression uncontrolled, driving benign retinomas into malignant retinoblastomas [8]. With the recent advances in genomic and epigenetic analysis methodologies, it has been reported that loss of function of the *RB1* gene is insufficient for the development of retinoblastoma. Some other candidate oncogenes (*MDM4* [Gene ID:4194; OMIM 602704], *KIF14* [Gene ID:9928; OMIM 611279], *MYCN* [Gene ID:4613; OMIM 164840], *CDH11* [Gene ID:1009; OMIM 600023], *DEK* [Gene ID:7913; OMIM 125264], *E2F3* [Gene ID:1871; OMIM 600427]) have been found to drive retinoblastoma progression through the genomic gain or loss or overexpression in gene expression [9].

The most common initial sign of retinoblastoma is leukocoria, followed by strabismus and proptosis [10]. No racial or gender predisposition has been found for the development of retinoblastoma. Patients with hereditary retinoblastoma have an increased risk for developing secondary malignancies, such as osteosarcoma, soft tissue sarcomas, and melanomas

Correspondence to: Peiquan Zhao, Department of Ophthalmology, Xinhua Hospital, Affiliated to Shanghai Jiao Tong University School of Medicine, No. 1665, Kongjiang Road, Shanghai, China, 200092; Phone: +86-13311620396; email: zhaopeiquan@xinhuamed.com.cn

[11,12]. Early detection and early treatment are important for successful preservation of life and vision of patients with retinoblastoma, and identification of causative mutations is essential to access the risk of tumor development in the relatives of patients with retinoblastoma [13,14].

Mutations in the *RB1* gene have been reported in patients from East Asia (Table 1). Two studies from Japan published in 1994 reported a detection rate of mutations in *RB1* in tumors of 58% with PCR-SSCP and direct genomic sequencing and 40% with Southern blotting and RT–PCR [15,16]. A study from South Korea reported a detection rate of mutations in the *RB1* gene of 71.4% in peripheral blood with RB1 exome sequencing and multiplex ligation-dependent probe amplification (MLPA) in 2012 [17]. In a Chinese population, Cheng et al. examined genomic DNA from peripheral blood samples and tumor tissue samples from 47 patients with retinoblastoma with a detection rate of 21% with PCR-SSCP-DNA sequencing [18]. The He study reported germline mutations in peripheral blood samples from 85 patients with retinoblastoma with a total detection rate of 47.1% with Sanger sequencing and MLPA [19]. Recently, Lan analyzed germline mutations in peripheral blood from a large-scale Chinese cohort with Sanger sequencing and methylation-specific MLPA and reported a detection rate of 41.7% (75/180) [20]. Most of the studies above were based on conventional detection methods, such as Sanger sequencing and MLPA, especially in China. In addition, none of the recent studies above mentioned the detection of low-level mosaic mutations in the *RB1* gene.

Low-level mosaic mutations, which mean mutations with a lower mutant frequency than 50%, always less than 20%, play a crucial role in pathogenesis of sporadic retinoblastoma. Allele-specific PCR (AS-PCR) and deep sequencing have been demonstrated to be efficient for detecting mutations with a mutant frequency of less than 20% as previously reported [21-23]. However, these methods are still difficult for frequent use as they are time-consuming. Sanger sequencing can cover the whole genomic regions of the *RB1* gene but is not powerful enough to identify low-level mosaic mutations.

Recently, targeted next-generation sequencing (NGS) has been demonstrated to be a rapid and effective strategy for detecting all types of mutations, in which only protein-coding regions of one or multiple specific genes are sequenced [24,25]. Therefore, the aim of the present study was to use custom panel-based targeted NGS to identify germline mutations in the *RB1* gene from 149 unrelated Chinese patients with retinoblastoma. At the same time, considering the limitation of confirmation of low-frequency variants (LFVs) with Sanger sequencing, we first used PCR-based deep NGS to confirm the LFVs as an addition. With targeted NGS, Sanger sequencing, PCR-based deep NGS, and MLPA, the detection rate of germline mutations was 48.3% (72/149), with 90.3% (56/62) in the bilateral cases and 18.4% (16/87) in the unilateral cases.

METHODS

Patients: A total of 149 unrelated probands with retinoblastoma and their parents were selected for this study from Xinhua Hospital affiliated with Shanghai Jiao Tong University School of Medicine, Shanghai, China, between 2017 and 2020. The clinical diagnosis of retinoblastoma was made by clinical examination and radiological investigations (CT/MRI) along with Retcam imaging at the hospital. All clinical information and blood samples used in this study were obtained with informed written consent from the families and in accordance with the Declaration of Helsinki.

DNA isolation: 2 ml of peripheral venous blood from each proband and the proband's families was drawn into an anticoagulant tube containing EDTA, stored at -20 ºC prior to use. Genomic DNA was extracted with the High Pure PCR template preparation kit (Roche Diagnostics, Pleasanton, CA) in accordance with the manufacturer's protocol as previously described [26]. Each DNA sample was accurately quantified with the Qubit Quantification Platform (Invitrogen, Paisley, UK) or the NanoDrop 2000 spectrophotometer (Thermo Scientific, Waltham, MA).

DNA library preparation and targeted next-generation sequencing: Blood samples of all probands were subjected to targeted NGS. DNA libraries were prepared using the Illumina standard protocol. The amplified DNA was captured with custom panel-based targeted region–related biotinylated oligoprobes provided by the GenCap Enrichment Kit (MyGenostics, Beijing, China) or Agilent's SureSelect Library Prep Kit (Amplicon-gene, Shanghai, China). The panel was designed to contain the 27 exons and flanking intronic sequence of the *RB1* gene. Briefly, 3 μg of genomic DNA from each sample was fragmented for 350- to 400-bp products with nebulization, and Illumina adapters were then ligated to the fragments, which were then amplified with PCR. Libraries were prepared, and then the captured regions were enriched using the methods above according to the manufacturer's protocol. The enrichment process was validated with the Agilent 2100 Bioanalyzer (Agilent Technologies, Palo Alto, CA). Quantitative PCR were used to check the quantity of the library. The enrichment libraries were finally sequenced on an Illumina NextSeq 500 sequencer (MyGenostics) for paired read 2 × 100 bp or Illumina MiSeq (Amplicon-gene) for paired read 2 × 150 bp.

Table 1. Detection of RB1 mutations reported from different countries of East Asia.

Authors	Countries	Methods	Samples	Total number of RB patients	Total detection rates of mutations	Detection rates of mutations in bilateral RB
Takashi Shimizu et al.,1994 [15]	Japan	PCR-SSCP and direct genomic sequencing	Tumors	24	58%	50%
Mitsuo V. Kato et al., 1994 [16]	Japan	Southern blotting and RT–PCR	Tumor tissues and skin biopsies	10	40%	40%
SH Seo et al., 2012 [17]	South Korea	RB1 Exome sequencing and MLPA	Peripheral blood	21	71.4%	93.8%
Guangyin Cheng et al., 2013 [18]	China	PCR-SSCP-DNA sequencing	Peripheral blood and tumor tissues	47	21%	70%
Ming-yan He et al., 2014 [19]	China	DNA sequencing and MLPA	Peripheral blood	85	47.1%	92.3%
Xiaoping Lan et al., 2020 [20]	China	Sanger sequencing and MS-MLPA	Peripheral blood	180	41.7%	90.3%

Bioinformatics analysis: The raw sequence reads were mapped to the UCSC GRCh37/hg19 human reference genome using the Burrows–Wheeler Aligner (BWA, V 0.7.11). The sequence of the *RB1* gene (accession number L11910) was used as reference. Variants were locally realigned with the GenomeAnalysisTK (GATK, V 3.3) toolkit and identified using ANNOVAR based on the Human Gene Mutation Database (HGMD), ClinVar, ExAC, ESP, and the 1000 Genomes project. Multiple bioinformatics tools, including PROVEAN, SIFT, PolyPhen-2, MutationTaster, GERP++, and REVEL, were used to predict the pathogenicity of genetic variants. The pathogenicity of genetic variants were finally accessed according to the 2015 American College of Medical Genetics and Genomics (ACMG) and the Association for Molecular Pathology (AMP) guidelines [27]. The gene variant nomenclature was in accordance with the Human Genome Variation Society (HGVS) recommendations.

Confirmation of mutations with Sanger sequencing, PCR-based deep NGS, and MLPA: All single nucleotide variations (SNVs) and small insertions/deletions (InDels) detected in probands and their parents were subjected to Sanger sequencing. Genomic DNA was extracted using the method above. Primers flanking each variant were designed. The corresponding exons of the variants were amplified with PCR and purified according to the preset program in the Beckman automated workstation (Beckman Coulter Inc., Melville, MA). Purified PCR products were analyzed on a 3130XL Genetic Analyzer (Life Technologies, Carlsbad, CA). If the result of the Sanger sequencing of an LFV detected with targeted NGS was negative, then PCR-based deep NGS was conducted for added confirmation. In the PCR-based deep NGS, the only difference with targeted NGS was the amplified DNA that was a 200-bp-long sequence flanking the specific variant detected with targeted NGS rather than all the DNA fragments. All potential copy number variations (CNVs) in probands were further confirmed with MLPA. MLPA was strictly performed according to the formal protocol of the manufacturer with the SALSA MLPA kit P047-RB1 (MRC-Holland, Amsterdam, the Netherlands). Data were analyzed with Coffalyser software (MRC-Holland) downloaded from the MLPA website.

Statistical analysis: Statistical software (SPSS v.22; IBM Corp., Armonk, NY) was used for data analysis. One-way analysis of variance (ANOVA) and the chi-square test were performed to compare the differences between continuous or categorical variables. A p value of less than 0.05 was considered statistically significant.

RESULTS

This study included 149 probands with retinoblastoma (85 male patients (57%) and 64 female patients (43%), 87 unilateral cases (58.4%) and 62 bilateral cases (41.6%)) from a Chinese cohort with targeted NGS (Appendix 1). The general clinical profiles of this cohort are summarized in Table 2. Germline mutations were found in 72 probands (16 unilateral and 56 bilateral). The total detection rate was 48.3% (72/149), with a detection rate of 90.3% (56/62) in the bilateral cases and 18.4% (16/87) in the unilateral cases. The mean age at diagnosis of the probands was 13.0±1.30 months (mean ± standard error of the mean [SEM]) in the positive group and 27.1±2.30 months in the negative group. The majority of probands were classified into Group D or E (the International Intraocular Retinoblastoma of Classification, IIRC) at diagnosis, accounting for 95.8% in the positive group and 100% in the negative group.

In this study, 64 SNVs and small InDels, which consisted of 25 nonsense, 20 splicing, ten frameshift, eight missense, and one synonymous variants, were identified in 41.6% (62/149) of the samples (Table 3). The most common type of variant was nonsense, followed by splicing and frameshift variants, representing 39.1% (25/64), 31.3% (20/64), and 15.6% (10/64), respectively. In addition, ten CNVs, which included nine large deletions and one large duplication, were identified in the remaining ten probands. Mean age at diagnosis of probands with splicing variants was less than 12 months, while probands with missense variants had the oldest mean age at diagnosis (17.3±4.10 months) in this study. Early stages at diagnosis of retinoblastoma were rare; two were splicing variants, and one was CNV. The mean age at diagnosis and the laterality were compared among different types of mutations, which were not statistically significantly different (one-way ANOVA and the chi-square test).

The SNVs and InDels were comprised of 40 known and 24 novel variants, identified in 48 bilateral and 14 unilateral cases (Table 4). Of them, 55 were pathogenic, four were likely pathogenic, and five were of uncertain significance. The pathogenic variants were comprised of 45 substitutions, eight small deletions, and two small insertions, including 24 nonsense, 19 splicing, nine frameshift, and three missense variants. Of the pathogenic variants, 46 variants were de novo, seven were inherited from the father, one was inherited from the mother, and one was unavailable. Specifically, 83.3% (20/24) of the pathogenic nonsense variants were due to C to T transitions, and 85% (17/20) of them were located at the CGAarg codon of the *RB1* gene. The likely pathogenic variants included one missense, one nonsense, one frameshift, and one splicing variants. Of them, one was de novo,

Table 2. General clinical profiles of retinoblastoma probands in this study.

Characteristics	Positive (n=72)	Negative (n=77)
Age (months)	13.0±1.3	27.1±2.3
Sex (n)		
Male (%)	43(28.8)	42(28.2)
Female (%)	29(19.5)	35(23.5)
Laterality (n)		
Unilateral (%)	16(10.7)	71(47.7)
Bilateral (%)	56(37.6)	6(4.0)
IIRC Stage(n)		
A	1	0
B	1	0
C	1	0
D	25	35
E	44	42

Tumor exhibiting more advanced stage in one eye than the other is reported for bilateral patients. Positive: probands with RB1 mutations; Negative: probands without RB1 mutations.

and three were unavailable. The missense variant c.137G>A affected codon 46 of the *RB1* mRNA, changing the amino acid arginine to lysine. It fell at the last nucleotide of exon 1, which may affect the splice site of this exon. The other three likely pathogenic variants were classified as likely pathogenic due to the lack of samples from the probands' mothers and inconsistent effects predicted by multiple algorithms. The variants of uncertain significance included four missense and one synonymous (splicing) variants, of which two missense variants were inherited from the father, one missense variant was inherited from the mother, and two were unavailable. The synonymous variant c.861G>A (p.Glu287=) fell at the last nucleotide of exon 8, which may cause aberrant splicing in published studies [28,29]. Because these variants were predicted to be neutral, tolerated, or benign by multiple algorithms, the variants were classified as variants of uncertain significance.

Of the 40 known variants, six variants (c.751C>T, c.763C>T, c.1399C>T, c.1654C>T, c.1666C>T, c.265–2A>G) were concurrent in two unrelated probands, one variant (c.1215+1G>A) was concurrent in three unrelated probands, and one variant (c.958C>T) was concurrent in four unrelated

Table 3. General clinical profiles of retinoblastoma probands by types of variants.

Characteristics	NS	SP	FS	MS	CNVs
Age (months)	13.4±1.9	10.1±1.7	12.0±5.4	17.3±4.1	15.3±3.3
Laterality (n)					
Unilateral	4	3	5	4	2
Bilateral	21	17	5	4	8
IIRC Stage (n)					
A	0	1	0	0	0
B	0	0	0	0	1
C	0	1	0	0	0
D	11	6	3	2	3
E	14	12	7	8	6

Tumor exhibiting more advanced stage in one eye than the other is reported for bilateral patients. Probands had two different variants were calculated as two probands. Synonymous variants were not included. FS: Frameshift NS: Nonsense SP: Splicing MS: Missense CNVs: Copy number variations. Mean age at diagnosis was not different among patients with five types of variants by One-way ANOVA (F=0.834, p=0.509). Laterality between different variant types (#nonsense, #splicing variants and #CNVs versus ##frameshift and ##missense variants) was not different by the chi-square test (χ^2=3.174,p=0.075).

Table 4. Summary of germline mutations identified in the RB1 gene by targeted NGS.

Sample ID	Laterality	Age at diagnosis (month)	Stage	Location	cDNA change	Protein change	Expected Effect	Heredity	Reference	Path
C170226C02501	U	58	d	Exon1	c.14dupC	p.R7Pfs*24	frameshift	de novo	12541220	P
19C095179	B	11	ce	Exon1	c.29_60del	p.A11Gfs*9	frameshift	de novo	novel	P
CA1261B	B	3	dd	Exon2	c.199delC	p.P67Qfs*9	frameshift	de novo	novel	P
CA1405B	B	11	ec	Exon2	c.236delA	p.E79Gfs*31	frameshift	de novo	24225018	P
18C044455	U	2	e	Exon11	c.1121_1122delCA	p.P374Rfs*2	frameshift	de novo	7795591	P
17C035200	U	17	e	Exon13	c.1249_1250del	p.R418Sfs*9	frameshift	de novo	17960112	P
CA1233B	B	1	db	Exon 16	c.1455_1456del	p.L486Ifs*5	frameshift	de novo	novel	P
19C043857	B	3	be	Exon22	c.2253_2254del	p.I752Yfs*4	frameshift	de novo	novel	P
17C060094	U	12	e	Exon22	c.2285_2286delAG	p.R763Tfs*31	frameshift	de novo	novel	P
17C060247	B	8	dd	Exon14	c.1345G>A	p.G449R	missense	de novo	17096365	P
17C038288	B	12	de	Exon14	c.1346G>T	p.G449V	missense	de novo	novel	P
19C005190	B	42	ec	Exon23	c.2489G>T	p.R830I	missense	de novo	novel	P
C170224C04001	B	4	dd	Exon4	c.485_486TC>AA	p.F162X	nonsense	de novo	novel	P
CA1407B	B	6	de	Exon2	c.227T>G	p.L76X	nonsense	de novo	novel	P
18C001347	B	10	de	Exon7	c.619C>T	p.Q207X	nonsense	NA	8776589	P
C170302C06501	B	13	dd	Exon8	c.751C>T	p.R251X	nonsense	de novo	7704558	P
CA1234B	B	31	ed	Exon8	c.751C>T	p.R251X	nonsense	de novo	7704558	P
17C038371	B	5	de	Exon8	c.763C>T	p.R255X	nonsense	de novo	7704558	P
CA1282B	B	13	be	Exon8	c.763C>T	p.R255X	nonsense	de novo	7704558	P
18C057245	U	30	d	Exon10	c.958C>T	p.R320X	nonsense	de novo	7704558	P
C170226C02601	B	3	ed	Exon10	c.958C>T	p.R320X	nonsense	de novo	7704558	P
CA1290B	B	13	de	Exon10	c.958C>T	p.R320X	nonsense	de novo	7704558	P
CA1296B	U	33	d	Exon10	c.958C>T	p.R320X	nonsense	de novo	7704558	P
ED0393B	B	12	dd	Exon11	c.1072C>T	p.R358X	nonsense	de novo	7795591	P
19C085034	B	17	eb	Exon14	c.1363C>T	p.R455X	nonsense	de novo	8651278	P
19C149616	U	20	d	Exon15	c.1399C>T	p.R467X	nonsense	de novo	7795591	P
CA1259B	B	9	dd	Exon15	c.1399C>T	p.R467X	nonsense	de novo	7795591	P
17C049460	B	6	ec	Exon17	c.1548G>A	p.W516X	nonsense	de novo	novel	P
CA1284B	U	3	e	Exon17	c.1654C>T	p.R552X	nonsense	father	7704558	P
CA1351B	B	27	ea	Exon17	c.1654C>T	p.R552X	nonsense	father	7704558	P
C170209C00101	B	3	db	Exon17	c.1666C>T	p.R556X	nonsense	de novo	7704558	P

Sample ID	Laterality	Age at diagnosis (month)	Stage	Location	cDNA change	Protein change	Expected Effect	Heredity	Reference	Path
CA1309B	B	8	bd	Exon17	c.1666C>T	p.R556X	nonsense	de novo	7704558	P
18C037953	B	18	ed	Exon18	c.1723C>T	p.Q575X	nonsense	father	8651278	P
CA1298B	B	8	db	Exon18	c.1735C>T	p.R579X	nonsense	de novo	7704558	P
19C019664	B	7	bd	Exon21	c.2127T>A	p.Y709X	nonsense	de novo	novel	P
19C149227	B	24	ed	Exon22	c.2284C>T	p.Q762X	nonsense	de novo	8776589	P
18C014696	B	6	bd	Intron1	c.138-1G>T		splicing	de novo	novel	P
CA1257B	B	2	da	Intron2	c.265-2A>G		splicing	de novo	15605413	P
CA1258B	B	2	aa	Intron2	c.265-2A>G		splicing	father	15605413	P
19C085025	B	12	ed	Intron5	c.540-1G>T		splicing	de novo	novel	P
18C014733	U	16	e	Intron6	c.608-2A>G		splicing	father	17960112	P
17C060140	U	13	e	Intron8	c.862-1G>A		splicing	father	24225018	P
19C043876	B	5	dd	Intron9	c.940-2A>G		splicing	de novo	22180099	P
19C043879	B	6	ac	Intron9	c.940-1G>T		splicing	de novo	novel	P
18C037993	B	1	eb	Intron10	c.1049+1G>A		splicing	de novo	novel	P
CA1422B	B	6	be	Intron11	c.1128-2A>T		splicing	de novo	novel	P
18C014515	B	14	d	Intron12	c.1215+1G>A		splicing	de novo	2601691	P
18C037965	B	4	ae	Intron12	c.1215+1G>A		splicing	de novo	2601691	P
18C014512	U	17	ce	Intron12	c.1215+1G>A		splicing	de novo	2601691	P
19C005097	B	30	eb	Intron13	c.1332+3A>C		splicing	mother	novel	P
ED0371B	B	10	dd	Intron15	c.1421+1G>A		splicing	father	novel	P
17C056558	B	5	be	Intron18	c.1814+3A>T		splicing	de novo	22963398	P
17C024351	B	22	ce	Intron20	c.2107-3T>G		splicing	de novo	novel	P
CA1335B	B	8	dc	Intron22	c.2326-1insCC		splicing	de novo	novel	P
ED0384B	B	5	ce	Intron24	c.2520+5G>A		splicing	de novo	15605413	P
18C014502	U	2	e	Exon16	c.1432dupA	p.N478Kfs*2	frameshift	NA	novel	LP
CA1283B	B	13	ec	Exon1	c.137G>A	p.R46K	missense	de novo	19390654	LP
18C057224	B	11	de	Exon22	c.2268T>A	p.Y756X	nonsense	NA	24688104	LP
CA1297B	B	18	ae	Intron15	c.1421+3A>T		splicing	NA	14769601	LP
17C024236	U	22	e	Exon2	c.197T>A	p.I66K	missense	father	novel	US
17C024236	U	22	e	Exon2	c.199C>G	p.P67A	missense	father	novel	US
17C060094	U	12	e	Exon9	c.920C>T	p.T307I	missense	mother	12541220	US
CA1251B	U	7	d	Exon10	c.1049G>C	p.S350T	missense	NA	novel	US

Sample ID	Laterality	Age at diagnosis (month)	Stage	Location	cDNA change	Protein change	Expected Effect	Heredity	Reference	Path
18C014668	B	22	ee	Exon8	c.861G>A	p.E287E	synonymous	NA	24225018	US

B: Bilateral U: Unilateral NA: Not Available Path: Pathogenicity P: Pathogenic LP: Likely Pathogenic US: Uncertain Significance

Molecular Vision 2021; 27:1-16 <http://www.molvis.org/molvis/v27/1>

probands (Table 4). All eight probands were classified into advanced retinoblastoma at diagnosis except proband CA1258B (c.265–2A>G). The unilateral retinoblastoma cases were diagnosed at a relatively older age than the bilateral cases with the same variant, whereas the difference in clinical stages at diagnosis between patients with the same variant was unclear.

The 24 novel variants were identified in 19 bilateral and four unilateral cases, with an average age at diagnosis of 10.9 months. The types of mutations included nine splicing, six frameshift, five missense, and four nonsense variants. Of them, 20 variants were pathogenic, one was likely pathogenic, and three were of uncertain significance (Table 5). Most novel variants were de novo and were predicted to be deleterious by PROVEAN, disease-causing by MutationTaster, and conserved by GERP++ tools. The frameshift variant c.1432dupA was classified as likely pathogenic due to the lack of samples from the probands' parents. The three missense variants were of uncertain significance as they were predicted to be benign by multiple bioinformatic tools. In addition, proband 17C024236, a 22-month-old male patient with a unilateral eye affected at diagnosis, was found to carry two different novel variants.

There were 21 variants (20 bilateral and six unilateral) located at the regions encoding two conserved domains A (residue 393–572) and B (residue 646–772) of pRb, of which eight were nonsense, six splicing, five frameshift, and two missense variants (Figure 1). The pathogenicity analysis indicated that 85.7% (18/21) of these variants were pathogenic, and the other three were likely pathogenic (c.1421+3A>T, c.1432dupA, c.2268T>A). The three variants were classified as likely pathogenic due to the absence of samples from the probands' parents, although c.2268T>A was predicted to be disease-related by multiple algorithms.

The mutant frequency was defined as the ratio of the total reads of mutant alleles to the total reads of wild-type alleles for the SNVs and InDels in the leukocyte DNA. Less than 20% of mutant frequency with targeted NGS was defined as LFVs. A total of eight variants (three bilateral and five unilateral) were identified as LFVs ranging from 3.39% to 19.0%, including four nonsense, three frameshift, and one splicing variants (Table 6). Six of the eight LFVs were identified with Sanger sequencing and two with PCR-based deep NGS (Figure 2), with a mutated frequency of 13.16% and 3.000%, respectively. Five of the LFVs were known, and three (c.2285_2286delAG, c.227T>G, c.1432dupA) were novel. Seven de novo LFVs were classified as pathogenic, while the variant c.1432dupA was likely pathogenic due to the lack of samples from the mother.

CNVs were identified in eight probands with bilateral retinoblastoma and two probands with unilateral retinoblastoma (Table 3); none of these probands' parents were subjected to genetic testing. All CNVs detected were further confirmed with MLPA (Table 7). The ratios of detection ranged from 0.32 to 0.69 for the large deletions and from 1.42 to 1.59 for a large duplication. The proband with deletion of exons 1 and 2 was a girl with early stages of bilateral retinoblastoma at the age of 1 month at diagnosis. Her mother was bilaterally affected by retinoblastoma. The proband with deletion of exons 1–23 was a girl who was 34 months old at diagnosis of unilateral retinoblastoma, whose mother was unilaterally affected. Four probands with bilateral retinoblastoma and one proband with unilateral retinoblastoma were found to have deletions of the whole *RB1* gene. Deletion of exons 1–17 were identified in a 2-month-old girl with bilateral retinoblastoma, and duplications of exons 18–23 were carried by a 13-month-old boy with bilateral retinoblastoma.

Three probands with bilateral retinoblastoma with different splicing variants were familial in this study (Figure 3). The disease–eye ratios (DERs) of these probands were 1.67, 2.00, and 1.50, all indicating a high disease penetrance (≥1.5). Variant c.265–2A>G was known and damaged the splice site between exon 2 and exon 3. However, another proband (RB99) with the same variant was de novo and had no similar family history. The other two splicing variants were novel, and both affected the probands bilaterally, which broke the splice sites between exons coding domain A. The variant of proband RB54 (c.1332+3A>C) was inherited from his mother who was unilaterally affected, and his sister was also affected. The variant of proband RB145 (c.1421+1G>A) was inherited from his father who was unilaterally affected.

DISCUSSION

NGS is increasingly used in gene mutation analysis of retinoblastoma. The utilization of targeted NGS makes the sequencing cost lower and the sequencing more efficient and convenient. Screening of mutations in the *RB1* gene with targeted NGS substantially benefits the prepotency, early diagnosis, and treatment of retinoblastoma. If the mutations in *RB1* are hereditary, the parents will be advised to have a second baby through in vitro fertilization techniques or early prenatal diagnosis for high-risk offspring. If the mutations in *RB1* are not found in patients or are nonhereditary, the parents will not be worried about having a second baby, and the follow-up period for patients could be extended. In general, targeted NGS is popular in genetic sequencing of retinoblastoma for ophthalmologists and geneticists.

Table 5. Novel mutations identified in the RB1 gene.

Sample ID	cDNA change	Protein change	PROVEAN	SIFT	PolyPhen_2	MutationTaster	GERP++	REVEL	ClinVar	Path
19C095179	c.29_60del	p.A11Gfs*9	-	-	-	-	-	-	-	P
CA1261B	c.199delC	p.P67Qfs*9	-	-	-	-	-	-	-	P
CA1233B	c.1455_1456del	p.L486Ifs*5	-	-	-	-	-	-	-	P
19C043857	c.2253_2254del	p.I752Yfs*4	-	-	-	-	-	-	-	P
17C060094	c.2285_2286delAG	p.R763Tfs*31	-	-	-	-	-	-	-	P
17C038288	c.1346G>T	p.G449V	Deleterious	D	Probably damaging	Disease_causing	Con	0.921	P	P
19C005190	c.2489G>T	p.R830I	Deleterious	D	Probably damaging	Disease_causing	Con	0.81	-	P
CA1407B	c.227T>G	p.L76X	Deleterious	-	-	Disease_causing	Con	-	-	P
C170224C04001	c.485_486TC>AA	p.F162X	Deleterious	-	-	Polymorphism	Con	0.126	-	P
17C049460	c.1548G>A	p.W516X	Deleterious	-	-	Disease_causing	Con	-	-	P
19C019664	c.2127T>A	p.Y709X	Deleterious	-	-	Disease_causing	Con	-	-	P
18C014696	c.138-1G>T		-	-	-	Disease_causing	Con	-	-	P
19C085025	c.540-1G>T		-	-	-	Disease_causing	Con	-	-	P
19C043879	c.940-1G>T		-	-	-	Disease_causing	Con	-	LP	P
18C037993	c.1049+1G>A		-	-	-	Disease_causing	Con	-	LP	P
CA1422B	c.1128-2A>T		-	-	-	Disease_causing	Con	-	-	P
19C005097	c.1332+3A>C		-	-	-	-	-	-	-	P
ED0371B	c.1421+1G>A		-	-	-	Disease_causing	Con	-	-	P
17C024351	c.2107-3T>G		-	-	-	-	-	-	-	P
CA1335B	c.2326-1insCC		-	-	-	-	-	-	-	P
18C014502	c.1432dupA	p.N478Kfs*2	-	-	-	-	-	-	-	LP
17C024236	c.197T>A	p.I66K	Neutral	D	Benign	Disease_causing	Con	0.471	-	US
17C024236	c.199C>G	p.P67A	Neutral	T	Benign	Disease_causing	Con	0.243	-	US
CA1251B	c.1049G>C	p.S350T	Neutral	T	Benign	Disease_causing	Con	-	-	US

D: Damaging T: Tolerated Con: Conserved LP: Likely Pathogenic P: Pathogenic US: Uncertain_significance Path: Pathogenicity.

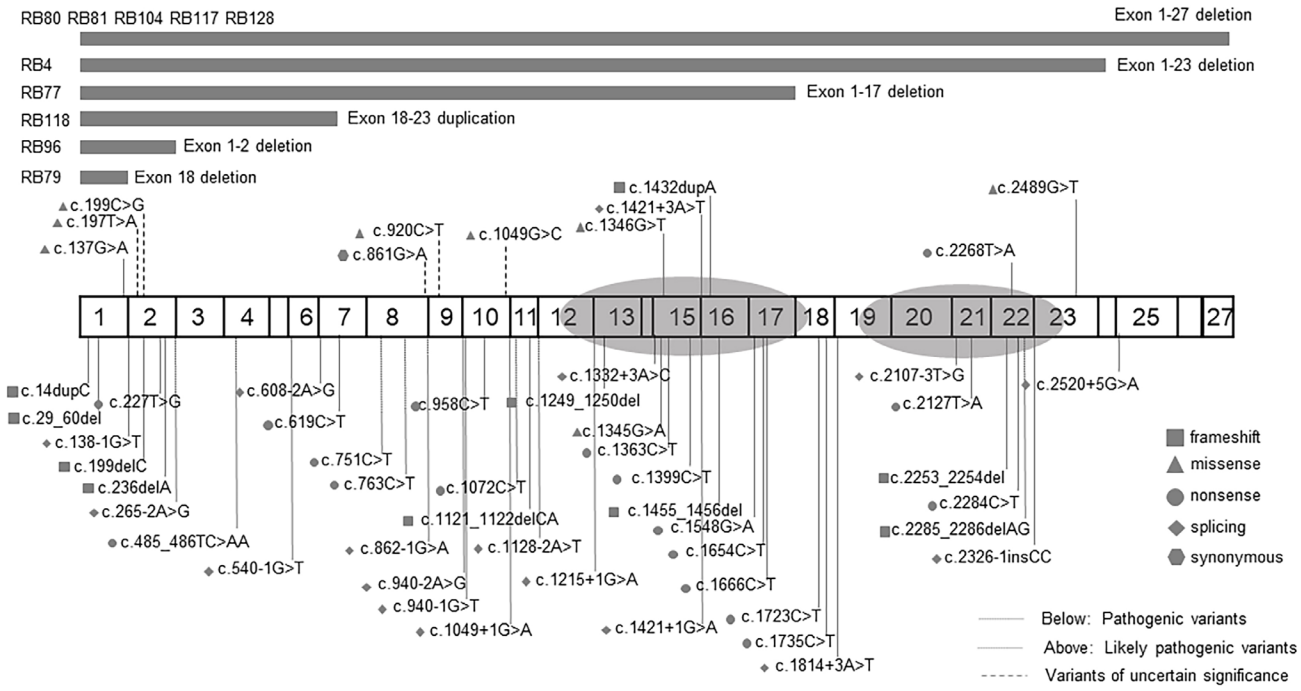

Figure 1. The distribution of detected mutations in the RB1 gene. Mutation types in the 27 exons and splice sites of the gene are described. The two oval grey regions represent the functional domains A and B; the numbers in boxes refer to the exons. The five symbols denote five various mutation types; the lines above or below the gene schematic refer to 3 types of pathogenicity of mutations. Copy number variations (CNVs) of the RB1 gene are presented as the grey bars.

In this study, we reported 64 distinct germline SNVs and InDels and ten distinct CNVs in 72 probands from a cohort of 149 unrelated Chinese patients with retinoblastoma using targeted NGS. The total detection rate in this study was 48.3%, which is within the reported range of rates of 42.0–67.0% with Sanger sequencing and MLPA [20,30]. The detection rate of 90.3% in the probands with bilateral retinoblastoma is also consistent with previous reports (88.8–100%) [20,31,32]. The detection rate was relatively not that high, which may be due to the limitation of the panel designed in this study to report mutations in the promotor region or deep intronic variants which were actually uncovered. In addition, in this study, two variants were confirmed using PCR-based deep NGS rather than Sanger sequencing, which improved the detection rate from 47.0% (70/149) to 48.3% (72/149). To the best of our knowledge, this is the first report to combine the three methods of targeted NGS, Sanger sequencing, and

Table 6. Low-frequency variants identified by targeted NGS.

Sample ID	cDNA change	Mutant frequency by targeted NGS	Mutant frequency by deep NGS	Sanger sequencing
18C014512	c.1215+1G>A	173/33(16%)	11,280/1485(13%)	-
19C149227	c.2284C>T	598/21(3.39%)	48,738/1628(3%)	-
18C044455	c.1121_1122delCA	140/33(19%)	/	+
17C060094	c.2285_2286delAG	405/55(12%)	/	+
CA1407B	c.227T>G	412/65(14%)	/	+
CA1284B	c.1654C>T	107/16(13%)	/	+
CA1309B	c.1666C>T	584/122(17%)	/	+
18C014502	c.1432dupA	111/18(14%)	/	+

The mutant frequency is based on the ratio of the total reads of the mutant and wild-type alleles.

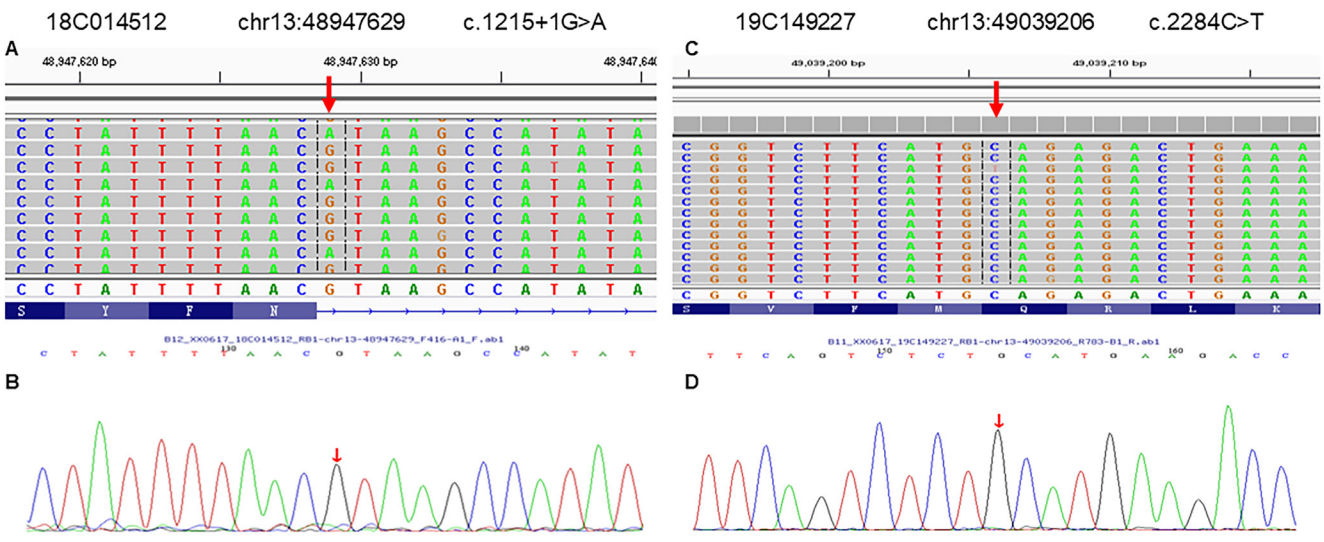

Figure 2. The sequencing results of the two probands with low-frequency variants (18C014512 and 19C149227). **A**, **C**: The mutated nucleotide sites (red arrows) were showed by the sequencing of PCR-based deep NGS platform. **B**, **D**: Only single peaks were showed at the nucleotide sites (red arrows) in the chromatograms of Sanger sequencing.

PCR-based deep NGS for identification of low-frequency variants in the *RB1* gene.

The general clinical findings of the probands in this study were similar to those for the distribution of Chinese patients with retinoblastoma reported previously [12,19]. Moreover, the number of probands with advanced retinoblastoma (IIRC D or E stage) at diagnosis was higher than 95% in this cohort, suggesting the severe condition of retinoblastoma at diagnosis in China. This may also be relevant to the fact that our hospital is a tertiary hospital in Shanghai, and diagnosis of patients with retinoblastoma who come to our hospital is often delayed. Additionally, we identified 40 known and 24 novel variants for SNVs and InDels, 53 of which were classified as pathogenic and six as likely pathogenic. The most common type of variant was nonsense, followed by splicing and frameshift variants. We found no statistically significant differences in the mean age at diagnosis and laterality among different types of mutations, which was as the same result as in Sagi's study in Israel [33]. However, the probands with missense variants tended to be older at diagnosis, and those with null mutations tended to have a younger average age at diagnosis. This perhaps could be explained by that missense mutations usually lead to reduction of function instead of loss of function of pRB. The familial cases, which were all splicing mutations, also revealed the high penetrance of splicing mutations as null mutations leading to the disruption of important splicing sites [19]. In Mehyer's

Table 7. CNVs identified by targeted NGS and MLPA methods.

Sample ID	NGS results	Ratio	MLPA results	Reference
17C024367	Exon1–23 deletion	0.32–0.53	Exon1–23 deletion	25,754,945
19C144823	Exon1–17 deletion	0.42–0.66	Exon1–17 deletion	23,301,675
19C149230	Exon18 deletion	0.51	Exon18 deletion	22,180,099
19C149232	Exon1–27 deletion	0.6–0.69	Exon1–27 deletion	12,541,220
19C149239	Exon1–27 deletion	0.47–0.57	Exon1–27 deletion	12,541,220
CA1244B	Exon1–2 deletion	0.47–0.54	Exon1–2 deletion	29,261,756
CA1281B	Exon1–27 deletion	0.48–0.62	Exon1–27 deletion	12,541,220
CA1357B	Exon1–27 deletion	0.5–0.57	Exon1–27 deletion	12,541,220
CA1325B	Exons duplication?	1.42–1.59	Exon18–23 duplication	26,530,098
CA1323B	Exon1–27 deletion	0.47–0.57	Exon1–27 deletion	12,541,220

study, splicing and frameshift mutations were associated with more advanced tumor stage [34], which was not found due to the rarity of patients diagnosed with an early stage of retinoblastoma in this cohort. As for the CNVs, all were identified with MLPA in the present study. Some patients may also have deletions or duplications of genes near the *RB1* gene, which needs more studies to explore their relationships with the phenotypes of patients with retinoblastoma [20].

Importantly, low-level mutational mosaicism is still a challenge for molecular diagnostics of retinoblastoma. Conventional methods are difficult for routinely detecting low-frequency mutant alleles in the *RB1* gene. It has been reported that Sanger sequencing is able to disclose mosaicism only for rates above 20% [21]. However, several previous studies reported more sensitive methods. Rushlow et al. identified low-level mosaicism in 5.5% of bilateral retinoblastoma cases with AS-PCR of 11 mutational "hot spots" [22].

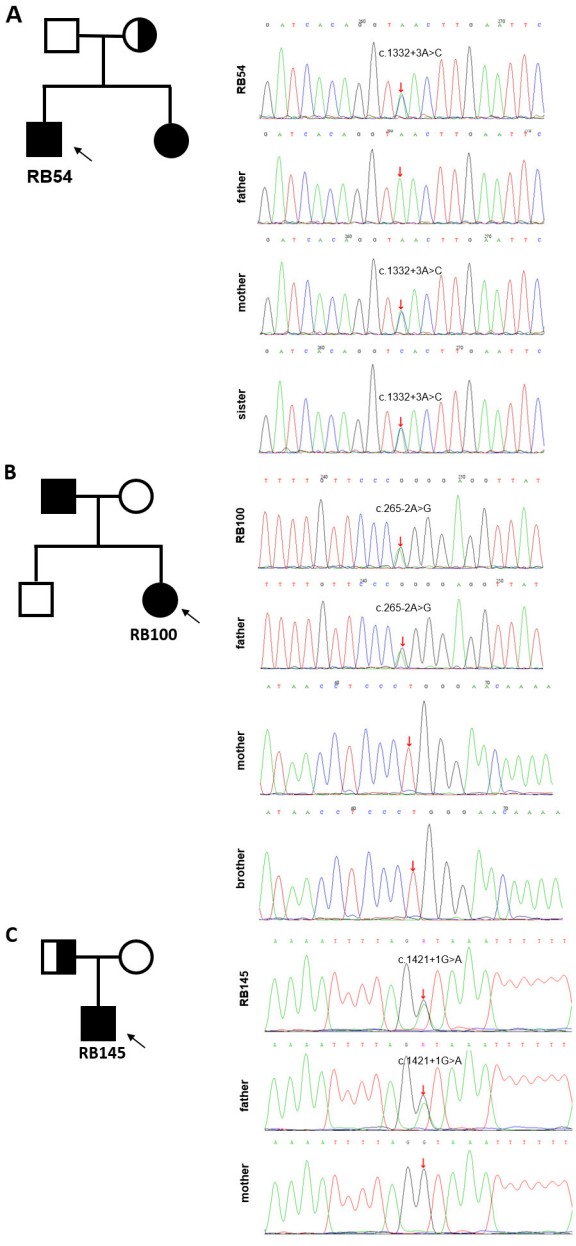

Figure 3. Pedigrees of three retinoblastoma familial cases. **A**: The mother's left eye and both eyes of the sister and the proband were affected by a splicing variant (c.1332+3A>C). **B**: Both eyes of the father and the proband were affected by a splicing variant (c.265-2A>G). **C**: The father's left eye and both eyes of the proband were affected by a splicing variant (c.1421+1G>A). Blackened symbols: bilateral RB; half-blackened symbols: unilateral RB.

Chen et al. reported that for retinoblastoma cases without mutations with Sanger sequencing, deep or next-generation sequencing technology of the *RB1* gene can detect 30% and 6% low-level *RB1* mosaic mutations in bilateral and unilateral cases, respectively [21]. Amitrano et al. identified with deep sequencing low-level mosaic mutations in sporadic retinoblastoma cases at a frequency between 8% and 24% in blood DNA [23]. Currently, targeted NGS, which has been reported in several recent studies, is considered a highly sensitive and efficient approach for the detection of genetic mutations [24,35]. Therefore, in this study, we noticed that the targeted NGS approach detected eight low-frequency variants with mutant frequency of less than 20%; six of them were identified with Sanger sequencing, but two were not. For the other two low-frequency variants not validated with Sanger sequencing, we performed targeted NGS and PCR-based deep NGS. We believe that the occurrence rate of the same NGS error at the same variant site in the two NGSs was very low. In addition, the coverage of PCR-based deep NGS was much higher than the targeted NGS ([11,280/1485 and 48,738/1628] and [173/33 and 598/21]), supporting the results of the NGS screening more validly.

However, although targeted NGS has good sensitivity and efficiency for the detection of mutations in *RB1* and even low-level mosaic mutations, this method still needs additional related studies to explore its accuracy for a specific detectable range of the mutant frequency of mutations. Sanger sequencing and MLPA are needed to confirm the NGS results. In addition, functional studies on specific mutations in *RB1* are needed to help understand the mechanism of pathogenesis of retinoblastoma.

Conclusions: In summary, targeted NGS is a cost-saving and efficient method for genetic sequencing of retinoblastoma. We identified 24 novel variants and eight low-frequency variants in the *RB1* gene with targeted NGS, which expanded the spectrum of mutations in *RB1* and may help improve the molecular diagnosis of retinoblastoma.

APPENDIX 1. GENERAL PROFILES OF ALL RETINOBLASTOMA PROBANDS IN THIS COHORT.

To access the data, click or select the words "Appendix 1."

ACKNOWLEDGMENTS

We thank the patients and families who consented to participate in this study. The study was supported by National Natural Science Foundation of China (81470642, 81770964).
Dr. Xunda Ji (jixunda@xinhuamed.com.cn) and Dr. Peiquan Zhao (zhaopeiquan@xinhuamed.com.cn) are co-corresponding authors for this paper.

REFERENCES

1. Dimaras H, Kimani K, Dimba EA, Gronsdahl P, White A, Chan HS, Gallie BL. Retinoblastoma. Lancet 2012; 379:1436-46. [PMID: 22414599].
2. Houston SK, Murray TG, Wolfe SQ, Fernandes CE. Current update on retinoblastoma. Int Ophthalmol Clin 2011; 51:77-91. [PMID: 21139478].
3. Soliman SE, Racher H, Zhang C, MacDonald H, Gallie BL. Genetics and Molecular Diagnostics in Retinoblastoma–An Update. Asia Pac J Ophthalmol (Phila) 2017; 6:197-207. [PMID: 28399338].
4. Friend SH, Bernards R, Rogelj S, Weinberg RA, Rapaport JM, Albert DM, Dryja TP. A human DNA segment with properties of the gene that predisposes to retinoblastoma and osteosarcoma. Nature 1986; 323:643-6. [PMID: 2877398].
5. DiCiommo D, Gallie BL, Bremner R. Retinoblastoma: the disease, gene and protein provide critical leads to understand cancer. Semin Cancer Biol 2000; 10:255-69. [PMID: 10966849].
6. Dick FA, Rubin SM. Molecular mechanisms underlying RB protein function. Nat Rev Mol Cell Biol 2013; 14:297-306. [PMID: 23594950].
7. Hensey CE, Hong F, Durfee T, Qian YW, Lee EY, Lee WH. Identification of discrete structural domains in the retinoblastoma protein. N-terminal domain is required for its oligomerization. J Biol Chem 1994; 269:1380-7. [PMID: 8288605].
8. Dimaras H, Khetan V, Halliday W, Orlic M, Prigoda NL, Piovesan B, Marrano P, Corson TW, Eagle RC Jr, Squire JA, Gallie BL. Loss of RB1 induces non-proliferative retinoma: increasing genomic instability correlates with progression to retinoblastoma. Hum Mol Genet 2008; 17:1363-72. [PMID: 18211953].
9. Thériault BL, Dimaras H, Gallie BL, Corson TW. The genomic landscape of retinoblastoma: a review. Clin Experiment Ophthalmol 2014; 42:33-52. [PMID: 24433356].
10. Dimaras H, Corson TW, Cobrinik D, White A, Zhao J, Munier FL, Abramson DH, Shields CL, Chantada GL, Njuguna F, Gallie BL. Retinoblastoma. Nat Rev Dis Primers 2015; 1:15021-[PMID: 27189421].
11. Chen CS, Suthers G, Carroll J, Rudzki Z, Muecke J. Sarcoma and familial retinoblastoma. Clin Experiment Ophthalmol 2003; 31:392-6. [PMID: 14516425].
12. Zhao J, Li S, Shi J, Wang N. Clinical presentation and group classification of newly diagnosed intraocular retinoblastoma in China. Br J Ophthalmol 2011; 95:1372-5. [PMID: 21252083].
13. Vogel F. Genetics of retinoblastoma. Hum Genet 1979; 52:1-54. [PMID: 393614].

14. Fabian ID, Onadim Z, Karaa E, Duncan C, Chowdhury T, Scheimberg I, Ohnuma SI, Reddy MA, Sagoo MS. The management of retinoblastoma. Oncogene 2018; 37:1551-60. [PMID: 29321667].

15. Shimizu T, Toguchida J, Kato MV, Kaneko A, Ishizaki K, Sasaki MS. Detection of mutations of the RB1 gene in retinoblastoma patients by using exon-by-exon PCR-SSCP analysis. Am J Hum Genet 1994; 54:793-800. [PMID: 8178820].

16. Kato MV, Ishizaki K, Toguchida J, Kaneko A, Takayama J, Tanooka H, Kato T, Shimizu T, Sasaki MS. Mutations in the retinoblastoma gene and their expression in somatic and tumor cells of patients with hereditary retinoblastoma. Hum Mutat 1994; 3:44-51. [PMID: 8118465].

17. Seo SH, Ahn HS, Yu YS, Kang HJ, Park KD, Cho SI, Park JS, Hyun YJ, Kim JY, Seong MW, Park SS. Mutation spectrum of RB1 gene in Korean bilateral retinoblastoma patients using direct sequencing and gene dosage analysis. Clin Genet 2013; 83:494-6. [PMID: 22963398].

18. Cheng G, Wang Y, Bin L, Shi J, Zhao J, Jonas JB. Genetic and Epigenetic Profile of Retinoblastoma in a Chinese Population: Analysis of 47 Patients. Asia Pac J Ophthalmol (Phila) 2013; 2:414-7. [PMID: 26107153].

19. He MY, An Y, Gao YJ, Qian XW, Li G, Qian J. Screening of RB1 gene mutations in Chinese patients with retinoblastoma and preliminary exploration of genotype-phenotype correlations. Mol Vis 2014; 20:545-52. [PMID: 24791139].

20. Lan X, Xu W, Tang X, Ye H, Song X, Lin L, Ren X, Yu G, Zhang H, Wu S. Spectrum of RB1 Germline Mutations and Clinical Features in Unrelated Chinese Patients With Retinoblastoma. Front Genet 2020; 11:142-[PMID: 32218800].

21. Chen Z, Moran K, Richards-Yutz J, Toorens E, Gerhart D, Ganguly T, Shields CL, Ganguly A. Enhanced sensitivity for detection of low-level germline mosaic RB1 mutations in sporadic retinoblastoma cases using deep semiconductor sequencing. Hum Mutat 2014; 35:384-91. [PMID: 24282159].

22. Rushlow D, Piovesan B, Zhang K, Prigoda-Lee NL, Marchong MN, Clark RD, Gallie BL. Detection of mosaic RB1 mutations in families with retinoblastoma. Hum Mutat 2009; 30:842-51. [PMID: 19280657].

23. Amitrano S, Marozza A, Somma S, Imperatore V, Hadjistilianou T, De Francesco S, Toti P, Galimberti D, Meloni I, Cetta F, Piu P, Di Marco C, Dosa L, Lo Rizzo C, Carignani G, Mencarelli MA, Mari F, Renieri A, Ariani F. Next generation sequencing in sporadic retinoblastoma patients reveals somatic mosaicism. Eur J Hum Genet 2015; 23:1523-30. [PMID: 25712084].

24. Devarajan B, Prakash L, Kannan TR, Abraham AA, Kim U, Muthukkaruppan V, Vanniarajan A. Targeted next generation sequencing of RB1 gene for the molecular diagnosis of Retinoblastoma. BMC Cancer 2015; 15:320-[PMID: 25928201].

25. Aravind S, Ashley B, Mannan A, Ganapathy A, Ramesh K, Ramachandran A, Nongthomba U, Shastry A. Targeted sequencing of the DMD locus: A comprehensive diagnostic tool for all mutations. Indian J Med Res 2019; 150:282-9. [PMID: 31719299].

26. Li J-K, Li Y, Zhang X, Chen C-L, Rao Y-Q, Fei P, Zhang Q, Zhao P, Li J. Spectrum of Variants in 389 Chinese Probands With Familial Exudative Vitreoretinopathy. Invest Ophthalmol Vis Sci 2018; 59:5368-81. [PMID: 30452590].

27. Richards S, Aziz N, Bale S, Bick D, Das S, Gastier-Foster J, Grody WW, Hegde M, Lyon E, Spector E, Voelkerding K, Rehm HL. Standards and guidelines for the interpretation of sequence variants: a joint consensus recommendation of the American College of Medical Genetics and Genomics and the Association for Molecular Pathology. Genet Med 2015; 17:405-24. [PMID: 25741868].

28. Buratti E, Chivers M, Královicová J, Romano M, Baralle M, Krainer AR, Vorechovsky I. Aberrant 5′ splice sites in human disease genes: mutation pattern, nucleotide structure and comparison of computational tools that predict their utilization. Nucleic Acids Res 2007; 35:4250-63. [PMID: 17576681].

29. Zhang MQ. Statistical features of human exons and their flanking regions. Hum Mol Genet 1998; 7:919-32. [PMID: 9536098].

30. Rojanaporn D, Boontawon T, Chareonsirisuthigul T, Thanapanpanich O, Attaseth T, Saengwimol D, Anurathapan U, Sujirakul T, Kaewkhaw R, Hongeng S. Spectrum of germline RB1 mutations and clinical manifestations in retinoblastoma patients from Thailand. Mol Vis 2018; 24:778-88. [PMID: 30636860].

31. Rojanaporn D, Boontawon T, Chareonsirisuthigul T, Thanapanpanich O, Attaseth T, Saengwimol D, Anurathapan U, Sujirakul T, Kaewkhaw R, Hongeng S. Spectrum of germline RB1 mutations and clinical manifestations in retinoblastoma patients from Thailand. Mol Vis 2018; 24:778-88. [PMID: 30636860].

32. Tomar S, Sethi R, Sundar G, Quah TC, Quah BL, Lai PS. Mutation spectrum of RB1 mutations in retinoblastoma cases from Singapore with implications for genetic management and counselling. PLoS One 2017; 12:e0178776-[PMID: 28575107].

33. Sagi M, Frenkel A, Eilat A, Weinberg N, Frenkel S, Pe'er J, Abeliovich D, Lerer I. Genetic screening in patients with Retinoblastoma in Israel. Fam Cancer 2015; 14:471-80. [PMID: 25754945].

34. Mehyar M, Mosallam M, Tbakhi A, Saab A, Sultan I, Deebajah R, Jaradat I, AlJabari R, Mohammad M, AlNawaiseh I, Al-Hussaini M, Yousef YA. Impact of RB1 gene mutation type in retinoblastoma patients on clinical presentation and management outcome. Hematol Oncol Stem Cell Ther 2020; 13:152-9. [PMID: 32222358].

35. Singh J, Mishra A, Pandian AJ, Mallipatna AC, Khetan V, Sripriya S, Kapoor S, Agarwal S, Sankaran S, Katragadda S, Veeramachaneni V, Hariharan R, Subramanian K, Mannan AU. Next-generation sequencing-based method shows increased mutation detection sensitivity in an Indian

retinoblastoma cohort. Mol Vis 2016; 22:1036-47. [PMID: 27582626].